Applied Physics Letters

Anomalous open-circuit voltage from a high-T_c superconducting dynamo

Cite as: Appl. Phys. Lett. **108**, 122601 (2016); https://doi.org/10.1063/1.4943663
Submitted: 07 October 2015 . Accepted: 27 February 2016 . Published Online: 22 March 2016

C. W. Bumby, Zhenan Jiang, J. G. Storey, A. E. Pantoja, and R. A. Badcock

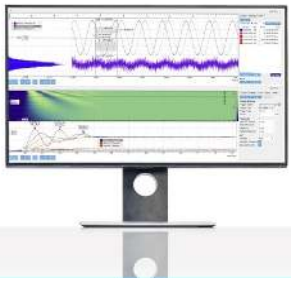

AIP Publishing

Anomalous open-circuit voltage from a high-T_c superconducting dynamo

C. W. Bumby,[a] Zhenan Jiang, J. G. Storey, A. E. Pantoja, and R. A. Badcock
Robinson Research Institute, Victoria University of Wellington, 69 Gracefield Road, Lower Hutt 5010, New Zealand

(Received 7 October 2015; accepted 27 February 2016; published online 22 March 2016)

We report on the behavior of a high-T_c superconducting (HTS) homopolar dynamo which outputs a DC open-circuit voltage when the stator is in the superconducting state, but behaves as a conventional AC alternator when the stator is in the normal state. We observe that this time-averaged DC voltage arises from a change in the shape of the AC voltage waveform that is obtained from a normal conducting stator. The measured DC voltage is proportional to frequency, and decreases with increasing flux gap between the rotor magnet and the HTS stator wire. We observe that the DC output voltage decreases to zero at large flux gaps, although small differences between the normal-conducting and superconducting waveforms are still observed, which we attribute to screening currents in the HTS stator wire. Importantly, the normalised pulse shape is found to be a function of the rotor position angle only. Based on these observations, we suggest that the origin of this unexpected DC effect can be explained by a model first proposed by *Giaever*, which considers the impact of time-varying circulating eddy currents within the HTS stator wire. Such circulating currents form a superconducting shunt path which "short-circuits" the high field region directly beneath the rotor magnet, at those points in the cycle when the rotor magnet partially overlaps the superconducting stator wire. This reduces the output voltage from the device during these periods of the rotor cycle, leading to partial rectification of the output voltage waveform and hence the emergence of a time-averaged DC voltage. © *2016 AIP Publishing LLC*. [http://dx.doi.org/10.1063/1.4943663]

Superconducting flux pumps[1–3] are a class of devices which induce a DC transport current to flow in a closed superconducting circuit. In recent times, a variety of flux pumps employing high-T_c superconductors (HTS) have attracted interest,[4–10] as these devices offer a promising route to reducing the cryogenic losses associated with metal current leads in an HTS magnet system. One such device is the HTS dynamo[1]—a type of rotating flux pump[6,11–13] in which one or more permanent magnets are mounted upon a rotor and traverse a high-T_c coated conductor wire in a periodic manner (see Fig. 1(a)). This action generates, a DC output voltage which drives a DC through a series-connected HTS coil.[13] This observation is rather surprising, as the topology of the HTS dynamo is identical to an AC homopolar generator, and should not deliver a DC emf. This expectation arises from Maxwell's third law (Faraday's law)

$$V(t) = -\iint \frac{d\mathbf{B}(\mathbf{r},t)}{dt} \cdot \mathrm{d}\boldsymbol{S}, \tag{1}$$

where $V(t)$ is the measured voltage around a filamentary conducting circuit loop at time t, $\mathbf{B}(\mathbf{r},t)$ is the local magnetic field vector at point $\mathbf{r}$ in space, and the integral $\iint d\boldsymbol{S}$ is the integral over the area enclosed by the circuit loop. When a periodic B-field, of frequency f, is applied, then the time-averaged output voltage, $\bar{V}$, is obtained from Equation (1) as

$$\bar{V} = f\int_0^{\frac{1}{f}} V(t)dt = -f\iint \left[\mathbf{B}\left(\mathbf{r}, t=\frac{1}{f}\right) - \mathbf{B}(\mathbf{r}, t=0)\right] \cdot d\boldsymbol{S}. \tag{2}$$

For any cyclical device, it must follow that $\mathbf{B}(\mathbf{r}, t = 1/f) = \mathbf{B}(\mathbf{r}, t = 0)$ at all points in space; hence, Equation (2) implies that $\bar{V}$ must always equal zero. Nonetheless, DC output voltages have been experimentally reported from a number of HTS dynamo devices.[6,11–15]

To explore this issue, we have built a simple experimental HTS dynamo and examined the open-circuit behaviour of

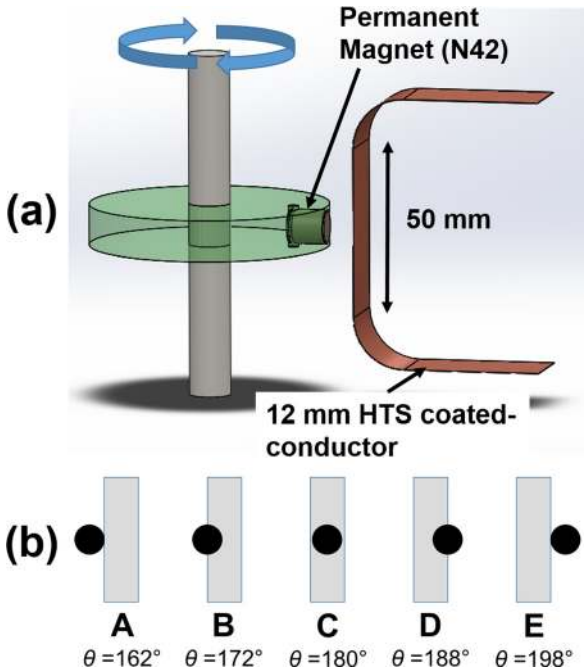

FIG. 1. (a) Schematic of HTS dynamo device studied in this work. (b) Plan view of the sequence of positions of the rotor magnet as it traverses the HTS stator wire.

[a]Author to whom correspondence should be addressed. Electronic mail: chris.bumby@vuw.ac.nz

this device whilst immersed in a liquid nitrogen bath. The HTS stator wire was a 12 mm wide coated-conductor wire[16] manufactured by Superpower, Inc. (SF12050), comprising a $\sim 1\,\mu$m film of $YBa_2Cu_3O_{7-x}$ (YBCO) deposited upon a 50 μm Hastelloy substrate and capped with a $\sim 2\,\mu$m layer of silver. The rotor (35 mm diameter) carried a single Nd-Fe-B (N42) cylindrical permanent magnet of 10 mm diameter. The magnet was located on the circumference of the rotor, with its axis of magnetisation aligned radially. The frequency, f, at which the magnet crossed the HTS stator wire was controlled by a servo-motor drive which was connected to the rotor by a fibreglass shaft. The flux gap, d, between the rotor magnet and HTS stator wire could be reproducibly altered using interchangeable spacer plates. Accurate phase-matching between data obtained at different temperatures was achieved using an additional datum sensor which provided a signal at a fixed rotor angle.

The inset of Fig. 2(a) shows an example of the open-circuit voltage waveform delivered by this device, $V(t)$. This comprises a series of sharp peaks which occur as the magnet crosses the stator, which are separated by a shallow return oscillation as the rotor magnet completes its rotation away from the stator wire. Figure 2(a) shows an enlarged section of the same open-circuit waveform, $V(t)$, plotted against the rotor position angle, θ. Two traces are shown for waveforms obtained at temperatures of 77 K and 293 K, respectively. At 77 K, the HTS stator is superconducting, whilst at 293 K normal conduction occurs through the metal substrate and coating layer of the wire. We have experimentally confirmed that the voltage waveform obtained from a non-superconducting 12 mm wide copper stator wire at 77 K closely matches the values obtained at 293 K. This reflects the fact that the Nd-Fe-B rotor magnet used here has the same magnetisation value[17] at 293 K and 77 K. As a result, comparison between these two temperatures shows the effect of changing from a normal-conducting to a superconducting stator whilst retaining an identical device geometry.

For the region $|180 - \theta| < 18°$, there is a clear difference between the voltage traces obtained in the superconducting and normal states. This corresponds to the section of the cycle in which the rotor magnet is passing directly over the HTS stator tape (i.e., positions A to E in Fig. 1(b)). At 77 K, the positive voltage peak centred at 180° is narrower and slightly higher in amplitude than the peak obtained at 293 K. The effect of this change in pulse-shape is to alter the value of the full-cycle voltage integral in Equation (2). We find that the time-averaged output voltage at 293 K, $\overline{V_{293K}} = 0$, but that this is no longer the case at 77 K. Instead, we obtain a non-zero value, in this case $\overline{V_{77K}} = -76\,\mu$V. This is indicated by the dotted horizontal line in Fig. 2(a). This effect is further illustrated in Fig. 2(b) which shows the cumulative integral, $\int V(t)dt$, over several cycles of the rotor. Each full rotation leads to an incremental increase in the magnitude of this integral at 77 K. In contrast, the cumulative integrated voltage at 293 K is a periodic function centred around zero.

Figure 3 shows the voltage waveforms obtained from our HTS dynamo when operated at a range of frequencies and flux gaps. $\overline{V_{77K}}$ is proportional to f (Fig. 3(a)), and the shape of the frequency-normalised waveform is the same at all frequencies when plotted as a function of rotor angle (Fig. 3(b)). These observations imply that the underlying cause of the net DC voltage is not due to the processes within the stator material which exhibit a fixed time constant. Fig. 3(d) shows that $\overline{V_{77K}}$ decreases as the flux gap, d, is increased. This reflects the corresponding decrease in the applied perpendicular magnetic field, $B_\perp$, at the stator. For flux gaps of $d \gtrsim 7$ mm, we find that $\overline{V_{77K}} \approx 0$, which occurs once the applied flux is excluded from the stator wire by screening currents.[13]

Measurements using additional voltage taps arranged along the stator have confirmed that the time-averaged DC voltage is only developed in the region of the stator closest to the magnet ($\lesssim$15 mm either side of the rotor magnet centre). The induced emf from the remainder of the loop formed by the wires connecting the voltmeter can be eliminated by considering the value $\Delta V(t) = V_{77K}(t) - V_{293K}(t)$. $\Delta V(t)$ then describes the difference in the voltage waveform obtained from the superconducting stator compared to an identical normal conducting stator. Figure 3(c) shows plots of $\Delta V/f$ for three different frequencies, whilst Fig. 3(f) shows the plots of $\Delta V(t)$ for a range of different flux gaps. In both these plots, we observe four distinct regions.

For $|180 - \theta| > 18°$, $\Delta V \approx 0$. This corresponds to the period during which the rotor magnet is away from the stator such that the B-field at the stator is uniform and approximately zero. For $162° < \theta < 172°$ (rotor positions A → B in Fig. 1(b)), and for $188° < \theta < 198°$ (D → E), ΔV is non-

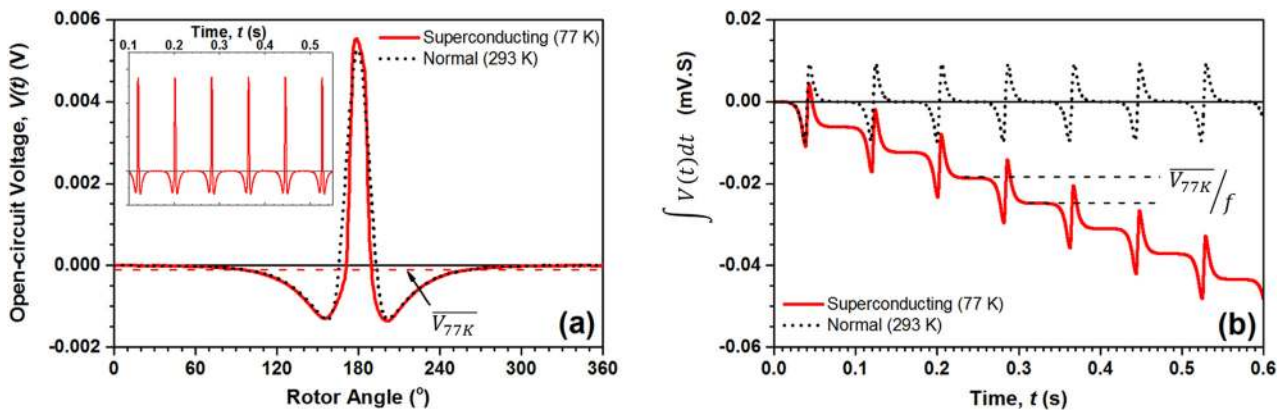

FIG. 2. (a) Inset: Example waveform of output voltage from HTS dynamo. Main figure: Expanded plot showing output voltage pulse versus rotor position. Data obtained at $f = 12.3$ Hz and $d = 3.3$ mm. (b) Integrated output voltage as function of time.

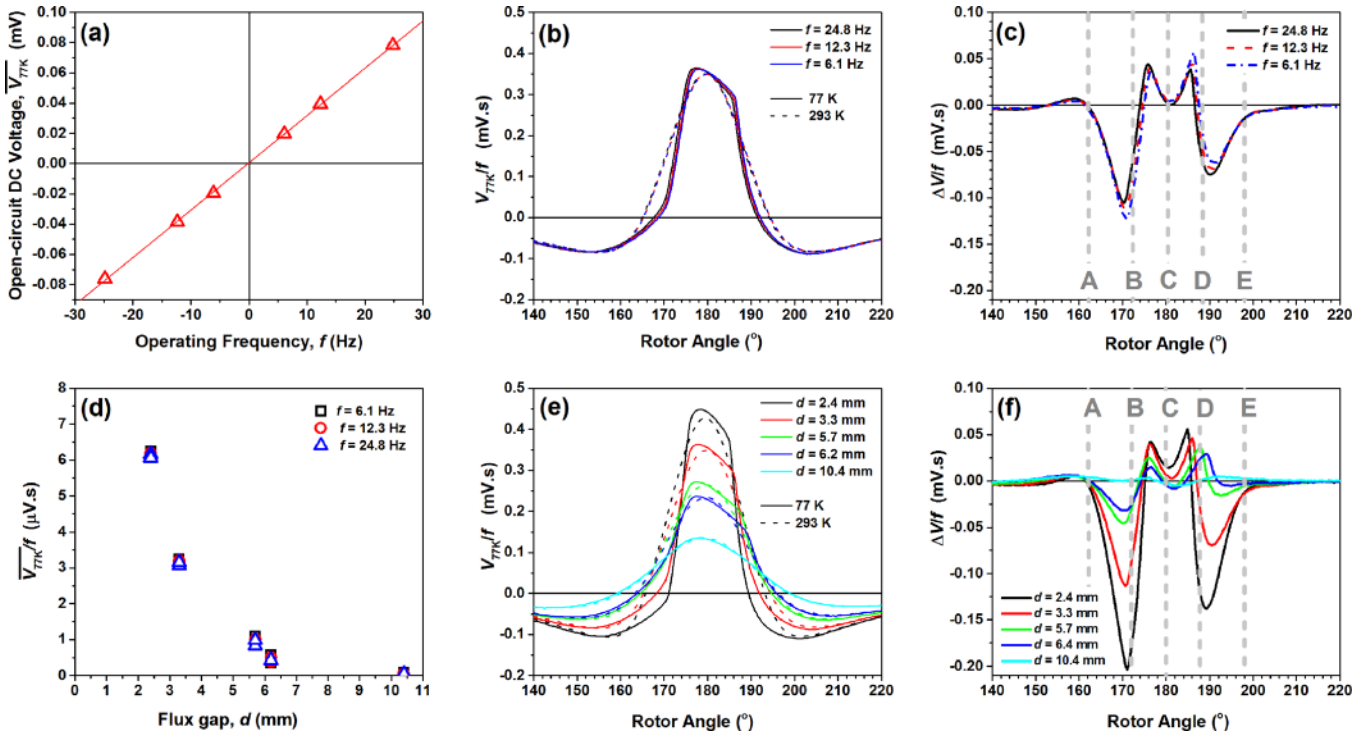

FIG. 3. (a) Measured open-circuit DC voltage, $\overline{V_{77K}}$, as a function of operating frequency (negative frequency indicates reverse motion of rotor). (b) Frequency-normalised output voltage, V_{77K}/f, versus rotor angle, θ, obtained at three different operating frequencies at a flux gap, d = 3.3 mm. (c) Frequency-normalised voltage difference, $\Delta V/f$, versus rotor angle, θ, for three different operating frequencies at a flux gap $d = 3.3$ mm. (d) Frequency-normalized DC voltage, $\overline{V_{77K}}/f$, obtained at different values of flux gap d at three different frequencies (in both forwards and reverse direction). (e) Frequency-normalised output voltage, V_{77K}/f, for different flux gaps at $f = 12.3$ Hz. (f) Frequency-normalised voltage difference, $\Delta V/f$ versus rotor angle, θ, at five different flux gaps at $f = 12.3$ Hz.

zero and negative. These two regions correspond to periods during which the rotor magnet partially covers the stator wire, but overlaps less than half the total wire width. For $172° < \theta < 188°$ (B → D), ΔV is small and positive. This corresponds to the period in which the rotor magnet is approximately centred above the coated-conductor wire.

Superconducting dynamos employing low-temperature superconductors (LTS) have been reported by various previous authors.[2,18–22] These devices utilise materials with a low B_{c2} such that a "normal-conducting spot" is considered to form in the high field region beneath the rotor magnet.[1] However, a normal spot is not formed in our HTS dynamo, as B_{c2} (at 77 K) of the YBCO coated conductor used in this work is much greater[23] than the applied rotor field of ~0.2 T. Instead, flux vortices will penetrate in the high field region beneath the rotor magnet and move through the HTS tape. *Giaever* has proposed a possible operating mechanism[24,25] for a unipolar superconducting DC generator which does not require a normal spot, and relies only on an increased local resistivity in the high magnetic field region. Flux flow causes dissipative loss[26,27] and therefore will give rise to an effective local resistivity in this region. In *Giaever's* model, superconducting eddy currents "short-circuit" the high field region during the passage of the rotor magnet across the stator. This means that the emf across this region is dropped across the effective internal resistance arising from the dissipative flux-flow. This leads to partial commutation of the output voltage, thus giving rise to a time-averaged DC voltage. We discuss the application of this model to our HTS dynamo below, and show that it can explain several key features of our experimental results.

Fig. 4(a) shows the circulating eddy currents which flow in the HTS stator tape for the idealised simple case of a square rotor magnet passing across the tape. Here we have assumed that the perpendicular magnetic field beneath the magnet $\overline{B}$ is constant, and the field elsewhere is zero (i.e.,

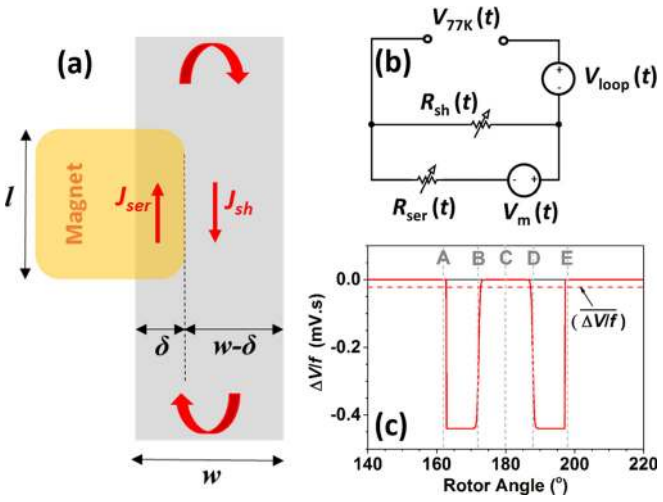

FIG. 4. (a) Schematic diagram illustrating circulating eddy currents in the HTS coated conductor wire as the rotor magnet passes over the stator. (b) Equivalent circuit which describes the effect of shunt leakage current path due to the circulating current. (c) Plot of Equation (7) for an idealized 10 mm × 10 mm square magnet operating at a flux gap of 1.5 mm, with $B_{\perp} = 0.2$ T and $n = 23$.

returning flux is screened from the interior of the HTS tape by shielding currents).

We expect that circulating eddy currents will flow along the wire as shown in Fig. 4(a). Under open-circuit conditions, the net sheet current flowing across a line transecting the wire must be zero, so we can state

$$\delta(\theta)\mathbf{J}_{ser} = -(w - \delta(\theta))\,\mathbf{J}_{sh}, \tag{3}$$

where $\delta(\theta)$ is the width of the overlap of the magnet above the HTS tape at rotor angle θ, within which an average local current density J_{ser} is induced in the "forward" direction (see Fig. 4(a)). Similarly, $w\text{-}\delta(\theta)$ is the width available for the returning "shunt" current, J_{sh}. It is important to note that Equation (3) does not hold for a normal-conducting stator wire as spreading resistance will restrict the spatial extent of normal eddy currents such that $\mathbf{J}_{\mathrm{sh}}$ does not extend across the full width of the available return path.

Flux-flow resistance in type-II HTS can be described by a power law relation of the form[28,29]

$$\mathbf{E} = E_0\left(\frac{|\mathbf{J}|}{J_c}\right)^n \hat{\mathbf{J}}, \tag{4}$$

where J_{c} is the critical current of the HTS wire at a threshold field of E_0, and n is a constant obtained by experiment. We can therefore define a local sheet resistivity,

$$\rho = \frac{E_0|\mathbf{J}|^{n-1}}{{J_{\mathrm{c}}}^n}. \tag{5}$$

The equivalent circuit shown in Fig. 4(b) describes the effect of a time-varying shunt leakage path on the measured open-circuit voltage. Here, $V_{\mathrm{m}}(t)$ represents the induced emf developed across the region directly beneath the rotor magnet and $V_{\mathrm{loop}}(t)$ denotes the emf induced in the wires which comprise the remainder of the measurement circuit, such that $V_{\mathrm{loop}}(t) = V_{293K}(t) - V_m(t)$.

From Equations (4) and (5), we can then express the effective resistance of the shunt leakage path as

$$R_{\mathrm{sh}} = \frac{l\rho_{sh}}{w - \delta} = \frac{lE_0|\boldsymbol{J}_{\mathbf{sh}}|^{n-1}}{(w - \delta){J_{\mathrm{c}}}^n}, \tag{6}$$

where l is the length of the shunt leakage path (see Fig. 4(a)). A similar expression can be obtained for the effective series resistance, R_{ser}.

Combining Equations (3) and (4) with a simple circuit analysis of Fig. 4(b), we can then state

$$\begin{aligned}\Delta V(t) &= V_{77K}(t) - V_{293K}(t) \approx V_{77K}(t) - \left[V_{\mathrm{loop}}(t) + V_{\mathrm{m}}(t)\right] \\ &= \frac{-V_{\mathrm{m}}(t)}{1 + \dfrac{R_{\mathrm{sh}}(t)}{R_{\mathrm{ser}}(t)}} \approx \frac{-V_{\mathrm{m}}(\theta)}{1 + \left(\dfrac{\delta(\theta)}{w - \delta(\theta)}\right)^n}.\end{aligned} \tag{7}$$

If l is the length of the square magnet and v is the speed at which the magnet is crossing the HTS stator wire, then we can approximate that $V_m = lv\overline{B}$ for $162° < \theta < 198°$ and is zero at all other times. From Equation (7), we then expect that $\Delta V(t)$ should equal zero when the rotor magnet is located away from the stator, and that the peak amplitude will be proportional to the speed (or frequency) at which the rotor magnet crosses the HTS stator wire. This is consistent with our experimental results.

Figure 4(c) shows a plot of Equation (7) for a square magnet with $l = 10$ mm and $n = 23$ (as measured for the stator in our experiment[16]), and $\overline{B} = 0.2$ T. We see that this plot shows qualitatively similar features to our experimental data (Figures 3(c) and 3(e)), with ΔV taking a negative value between points A → B and D → E, and being zero at all other times. This occurs because the ratio δ/(w-δ) changes as the rotor magnet moves across the stator wire. Between positions A → B and D → E of the rotor magnet, we find that $\delta < w\text{-}\delta$ and hence $R_{\mathrm{sh}} \ll R_{\mathrm{ser}}$. This means that the emf developed across the high field spot, $V_{\mathrm{m}}(t)$, is short-circuited during these periods of the cycle. As a result, $\Delta V = -V_{\mathrm{m}}$ and $V_{77\mathrm{K}}(t) = V_{293\mathrm{K}}(t) - V_{\mathrm{m}} = V_{\mathrm{loop}}(t)$. As the "short-circuit effect," only occurs during these two discrete sections of the cycle, this leads to partial rectification of the output voltage. It is clear from Figure 4(c) that $\overline{\Delta V/f} = \int_0^{360°}(\Delta V(\theta)/f)\,d\theta \neq 0$, and hence that this model will give rise to a net DC output voltage (as $\overline{\Delta V} = \overline{V_{77K}}$).

Equation (7) predicts that $\Delta V \approx 0$ between positions B → D (as $\delta > w\text{-}\delta$ and hence $R_{\mathrm{sh}} \gg R_{\mathrm{ser}}$). Experimentally, we actually observe a small positive value of ΔV throughout this section. A likely explanation is that during B → D, the magnet passes over the centre of the HTS tape and hence the circulating eddy currents within the stator wire must reverse direction (as the shunt return path moves from being in front of the high field spot to being behind it). This results in additional flux entering the tape thus causing an additional induced ac voltage to be measured. However, it is important to note that any such self-field effects within the stator wire are inherently periodic, and hence cannot give rise to a time averaged net DC field (from Equation (2)).

In conclusion, we have shown that the net DC output voltage from an HTS dynamo arises from a change in output ac waveform once the HTS stator enters the superconducting phase, and that this change in shape is qualitatively consistent with Giaever's model for a unipolar superconducting generator.[23] This mechanism is consistent with our experimental observations in which it leads to a pulse shape for $V(t)$ which is a function of θ only, and it predicts a value of $\overline{V_{77K}}$ which is both proportional to f and increases with the amplitude of the applied rotor field, B.

This work was supported by MBIE Contract No. RTVU1401. The authors would like to thank Shen Chong for his assistance with the temperature-dependent magnetisation measurements on the Nd-Fe-B rotor magnet. C.W.B. also wishes to thank Stuart Wimbush and Nick Long for their helpful comments during the preparation of this manuscript.

[1]L. J. M. van de Klundert and H. H. J. ten Kate, Cryogenics **21**, 195 (1981).
[2]H. Van Beelen, A. J. P. T. Arnold, H. A. Sypkens, J. P. Van Braam Houckgeest, R. de Bruyn Ouboter, J. J. M. Beenakker, and K. W. Taconis, Physica **31**, 413 (1965).
[3]K. Mendelssohn, Nature **132**, 602 (1933).
[4]R. M. Walsh, R. Slade, D. Pooke, and C. Hoffmann, IEEE Trans. Appl. Supercond. **24**, 4600805 (2014).

[5]W. Wang, F. Spaven, M. Zhang, M. Baghdadi, and T. Coombs, Appl. Phys. Lett. **104**, 032602 (2014).
[6]Z. Jiang, K. Hamilton, N. Amemiya, R. A. Badcock, and C. W. Bumby, Appl. Phys. Lett. **105**, 112601 (2014).
[7]T. Nakamura, M. Sugano, T. Doi, and N. Amemiya, IEEE Trans. Appl. Supercond. **20**, 1033 (2010).
[8]Z. Bai, C. Chen, Y. Wu, and Z. Zhen, Cryogenics **51**, 530 (2011).
[9]M. P. Oomen, M. Leghissa, G. Ries, N. Proelss, H. W. Neumueller, F. Steinmeyer, M. Vester, and F. Davies, IEEE Trans. Appl. Supercond. **15**, 1465 (2005).
[10]L. Fu, K. Matsuda, M. Baghdadi, and T. Coombs, IEEE Trans. Appl. Supercond. **25**, 4603804 (2015).
[11]C. Hoffmann, D. Pooke, and A. D. Caplin, IEEE Trans. Appl. Supercond. **21**, 1628 (2011).
[12]C. Hoffmann, R. Walsh, E. Karrer-Mueller, and D. Pooke, Phys. Proc. **36**, 1324 (2012).
[13]Z. Jiang, C. W. Bumby, R. A. Badcock, H.-J. Sung, N. Long, and N. Amemiya, Supercond. Sci. Technol. **28**, 115008 (2015).
[14]T. A. Coombs, J. F. Fagnard, and K. Matsuda, IEEE. Trans. Appl. Supercond. **24**, 1 (2014).
[15]C. W. Bumby, R. A. Badcock, H.-J. Sung, K.-M. Kim, Z. Jiang, A. E. Pantoja, P. Bernardo, M. Park, and R. G. Buckley, Supercond. Sci. Technol. **29**, 024008 (2016).
[16]See http://www.superpower-inc.com/system/files/SP_2G+Wire+Spec+Sheet_2014_web_v1_0.pdf for "2G HTS wire specifications" (last accessed 6 October 2015).
[17]See supplementary material at http://dx.doi.org/10.1063/1.4943663 for magnetisation data from Nd-Fe-B rotor magnet used in this work (Fig. S1).
[18]J. Volger and P. S. Admiraal, Phys. Lett. **2**, 257 (1962).
[19]K. Mawardi and S. Xu, IEEE Trans. Magn. **23**, 587 (1987).
[20]S. L. Wipf, in *Proceedings of the 1968 Summer Study On Superconducting Devices and Accelerators, Brookhaven, New York, USA* (1968), pp. 632–653.
[21]H. Tsukiji, K.-D. Choi, M. Tsukiyama, T. Nishiya, T. Hoshino, and E. Mukai, I. Muta. IEEE Trans. Appl. Supercond. **7**, 394 (1997).
[22]V. K. Kaplunenko, S. I. Moskvin, and V. V. Schmidt, Fiz. Nizk. Temp. **11**, 846 (1985).
[23]D. W. Hazelton and V. Selvamanickam, Proc. IEEE **97**, 1831 (2009).
[24]I. Giaever, IEEE Spectrosc. **3**, 117 (1966).
[25]I. Giaever, Phys. Rev. Lett. **15**, 825 (1965).
[26]Y. B. Kim, C. F. Hempstead, and A. R. Strnad, Phys. Rev. **139**, A1163 (1965).
[27]J. Geng and T. A. Coombs, Appl. Phys. Lett. **107**, 142601 (2015).
[28]T. Onogi, T. Ichiguchi, and T. Aida, Solid State Commun. **69**, 991 (1989).
[29]J. Rhyner, Physica C **212**, 292 (1993).